Investigation of Fragment Antibody Stability and Its Release Mechanism from Poly(Lactide-*co*-Glycolide)–Triacetin Depots for Sustained-Release Applications

DEBBY P. CHANG,[1] VIVEK KUMAR GARRIPELLI,[1] JENNIFER REA,[2] ROBERT KELLEY,[1] KARTHIKAN RAJAGOPAL[1]

[1]Drug Delivery Department, Genentech Inc., South San Francisco, California 94080
[2]Protein Analytical Chemistry Department, Genentech Inc., South San Francisco, California 94080

Received 16 March 2015; revised 14 May 2015; accepted 18 May 2015

Published online 22 June 2015 in Wiley Online Library (wileyonlinelibrary.com). DOI 10.1002/jps.24546

ABSTRACT: Achieving long-term drug release from polymer-based delivery systems continues to be a challenge particularly for the delivery of large hydrophilic molecules such as therapeutic antibodies and proteins. Here, we report on the utility of an *in situ*-forming and injectable polymer–solvent system for the long-term release of a model antibody fragment (Fab1). The delivery system was prepared by dispersing a spray-dried powder of Fab1 within poly(lactide-*co*-glycolide) (PLGA)–triacetin solution. The formulation viscosity was within the range 1.0 ± 0.3 Pa s but it was injectable through a 27G needle. The release profile of Fab1, measured in phosphate-buffered saline (PBS), showed a lag phase followed by sustained-release phase for close to 80 days. Antibody degradation during its residence within the depot was comparable to its degradation upon long-term incubation in PBS. On the basis of temporal changes in surface morphology, stiffness, and depot mass, a mechanism to account for the drug release profile has been proposed. The unprecedented release profile and retention of greater than 80% of antigen-binding capacity even after several weeks demonstrates that PLGA–triacetin solution could be a promising system for the long-term delivery of biologics. © 2015 Wiley Periodicals, Inc. and the American Pharmacists Association J Pharm Sci 104:3404–3417, 2015

Keywords: controlled release; PLGA; protein delivery; stability; spray drying; injectables

INTRODUCTION

The treatment of chronic back-of-the-eye diseases such as macular degeneration requires periodic intravitreal injections for sustaining the therapeutic benefit of drugs. Frequent injections are associated with poor patient compliance in disease treatment and can potentially damage the anatomical structure of the eye.[1] A sustained drug release system is therefore expected to overcome the complications associated with frequent injections by providing slow drug release for an extended duration from a single administration—typically for a few months. To achieve long-term drug release from a single dose, several sustained delivery systems such as solid implants,[2–4] injectable depots,[5–8] microparticles,[9,10] and specialized devices[3] are currently being investigated. An injectable sustained-release formulation is particularly beneficial because it can circumvent the need for invasive surgical procedures. For example, a millimeter-sized solid polymer implant may require a microsurgery or a specially designed syringe and needle for implantation, whereas an injectable formulation can be administered via a 27G or smaller bore needle.

Injectable sustained-release formulations can be designed in several forms, but non-aqueous polymer solution-based formulation is of interest here.[5] Dispersing the drug within an organic polymer solution produces such a formulation. Simply dissolving a bioresorbable and hydrophobic polymer such as poly(lactide-*co*-glycolide) (PLGA) in a biocompatible organic solvent such as N-methyl-2-pyrrolidone,[11,12] poly(ethyleneglycol) dimethyl ether,[13,14] triacetin,[15,16] or ethylbenzoate[17] produces the desired polymer solution. Upon injection of the drug-loaded organic polymer solution into aqueous environments, a stable depot is spontaneously formed because of demixing of the aqueous and nonaqueous phases. Depending on the solvent transfer rate to aqueous phase, the injected depot transitions to a solid material because of polymer precipitation while physically entrapping the drug included in the formulation. Water influx into the depot followed by polymer degradation is expected to control the drug release rate. Using this approach, several polymer–solvent combinations have been investigated for the sustained release of drugs ranging from small molecules and peptides to biologics.[14,18–23]

Herein, the utility of a non-aqueous polymer solution for the long-term delivery of large hydrophilic molecules such as fragment antibodies (Fab) has been investigated. Compared with small molecule drugs, proteins pose several challenges in the development of sustained-release formulations. Because of their larger size, the drug amount (on a molar basis) that can be accommodated within a delivery system is limited. Also, because of their inherent hydrophilicity, the diffusion-controlled release of proteins from sustained-release formulations is faster relative to small hydrophobic molecules. Therefore, the maximum release duration achieved for proteins from polymer solution-based formulations is only about a month.[8,19,20,24–26] Finally, maintaining the stability of a protein-based therapeutic during the formulation preparation process and long-term residence under physiological is a challenge in the development of drug delivery systems. The physicochemical "fragility" of protein-based therapeutics imposes severe limits on processing conditions and solvents that can be employed for formulation preparation.

Correspondence to: Karthikan Rajagopal (Telephone: +650-467-7326; Fax: +650-225-2764; E-mail: rajagopal.karthikan@gene.com)

This article contains supplementary material available from the authors upon request or via the Internet at http://wileylibrary.com.

Journal of Pharmaceutical Sciences, Vol. 104, 3404–3417 (2015)

The current study aims to investigate the protein release duration and its release mechanism from a polymer solution-based formulation. The effects of polymer physical properties and solvent nature on the phase inversion dynamics and drug release profiles have been reported in literature but the effect of polymer molecular weight and concentration on drug release remains unclear, particularly for large hydrophilic drug molecules. In addition, we have specifically focused on the physical and chemical changes that protein-based therapeutics can undergo during the formulation preparation process and during residence within the delivery system. To our knowledge detailed characterization of protein degradation has not been reported before. Also, knowledge of protein degradation pathways may be useful in overcoming stability issues through the selection of suitable excipients.

Using PLGA and triacetin as the polymer and solvent respectively, we have investigated the stability and *in vitro* release behavior of Fab1, a 48-kDa antibody fragment. Triacetin has been selected as the biocompatible organic solvent.[27] Triacetin is glycerin acetate. Upon hydrolysis, triacetin yields glycerol and acetic acid, molecules that are physiologically present and readily metabolized. Triacetin is a relatively less hydrophobic solvent (50 mg/mL aqueous phase solubility) but can dissolve a hydrophobic polymer such as PLGA. The preparation process and physical characterization of Fab1-loaded PLGA–triacetin formulation has been described. Next, the design of five different formulations to specifically examine the effects of PLGA concentration and its molecular weight on Fab1 release profile has been presented. On the basis of the *in vitro* release profiles, polymer degradation rates, temporal changes in depot microstructure, and its mechanical properties, a mechanism for Fab1 release from PLGA–triacetin depots has been proposed. Lastly, changes in Fab1 stability and its antigen-binding capacity were assessed at different stages during *in vitro* release.

EXPERIMENTAL

Materials

Fab1 was received from Genentech, Inc. (South San Francisco, California). PLGA polymers RG 752S, RG 755S, and RG 756S were purchased from Evonik Industries (Darmstadt, Germany) and labeled as PLGA-10k, PLGA-41k, and PLGA-56k, respectively. Triacetin (99%) was obtained from Acros Organics (Morris Plains, New Jersey). Coomassie Plus (Bradford) protein assay kit and NHS-Rhodamine was purchased from Thermo Fisher Scientific (Rockford, Illinois). D-Trehalose dihydrate was obtained from Ferro Pfanstiehl Laboratories (Cleveland, Ohio). Dichloromethane (DCM, 99.96%) was purchased from EMD Millipore Corporation (Billerica, Massachusetts). Tetrahydrofuran (THF, 99%) and polysorbate 20 (PS20) were purchased from Sigma–Aldrich (St. Louis, Missouri). All other chemicals were of analytical grade and used as received without further purification.

Spray Drying

Fab1 was formulated at 10 mg/mL in 10 mM histidine/histidine–HCl buffer at pH 5.5 containing 0.02% (w/w) PS20 and 10 mg/mL trehalose dihydrate. The aqueous Fab formulation was spray-dried using a B-191 Mini Spray Dryer (Buchi, New Castle, Delaware). The inlet temperature was set at 89 ± 2°C; with 100% aspirator capacity, atomizing air flow rate was set at 19.66 L/min and 10% liquid feed rate at 3.4 mL/min. This resulted in an outlet temperature of 59 ± 2°C. The spray-dried Fab1 powders were collected in a clean dry glass vial and stored under vacuum till further use.

Table 1. Formulation Details

Formulation	Polymer	PLGA Concentration (wt %)	Fab1 Loading (wt %)
Effect of PLGA Concentration			
A	PLGA-41k	7.5	1.5
B	PLGA-41k	10	1.5
C	PLGA-41k	12.5	1.5
Effect of PLGA MW			
F	PLGA-10k	10	1.5
B	PLGA-41k	10	1.5
G	PLGA-56k	10	1.5

Laser Diffraction Measurement of Particle Size Distribution

Spray-dried Fab1 particle size distribution was measured using a Horiba Partica LA-950V2 Laser Diffraction Particle Size Distribution Analyzer (Irvine, California). Approximately 20 mg of spray-dried Fab 1 powder was dispersed in 20 mL of isopropanol in a MiniFlow cell attached to the analyzer. The suspension was sonicated for 1 min prior to analysis. On the basis of scattering, the particle size distribution of a sample was analyzed (based on Mie scattering theory) using the refractive index (RI) of the particles (1.550) and the medium, isopropanol (1.3776). The volume-averaged size distribution was reported.

Scanning Electron Microscopy

The morphology of PLGA–triacetin depots and spray-dried drug particles were imaged with a Quanta 3D FEG scanning electron microscope (Hillsboro, Oregon). The depots were separated from release buffer and collected at different stages of release and freeze-dried prior to imaging. The freeze-dried depots were cut with a sharp razor blade to reveal the cross-sectional area. The samples were fixed on aluminum stubs with carbon adhesive tape and sputter coated with gold/palladium (Cressington Caron Coater; TED Pella Inc., Redding, CA) to improve their electrical conductivity. Scanning electron microscopy (SEM) images were collected at low voltage (5 kV) to minimize any potential sample damage or surface charging.

Water Content

Moisture content of the spray-dried particles was determined by volumetric Karl Fisher (KF) titration (DL31; Mettler-Toledo, Columbus, Ohio). Approximately 100 mg of spray-dried sample was injected into the titration cell with anhydrous methanol and Hydranal®-Composite 2 (Riedel-de Haen, Heidelberg, Germany) was used as the titrating reagent.

PLGA–Triacetin Formulation Preparation

A calculated quantity (see Table 1) of solid PLGA pellets were added to triacetin in a 7-mL glass vial and the contents were stirred using a magnetic stirrer at 400 rpm for 24 h to obtain a clear and transparent PLGA–triacetin solution. A calculated quantity (see Table 1) of spray-dried Fab1 powder was added to the PLGA–triacetin solution and the contents were stirred at 400 rpm for 24 h to obtain white and opalescent slurry.

Preparation of Rhodamine Conjugated Fab1

N-hydroxysuccinimide (NHS)-activated rhodamine (50 mg) was dissolved in 4 mL dimethyl sulfoxide (DMSO) and slowly added to 58 mL of Fab1 (34 mg/mL) in phosphate-buffered saline (PBS) taken in a vial. The contents were mixed at 4°C for 2 h and transferred to a dialysis cassette (MWCO 10 kDa). The contents of the dialysis cassette were dialyzed extensively against pH 5.5 buffer containing 10 mM histidine/histidine–HCl buffer. Purified rhodamine-conjugated Fab1 was recovered from the cassette and spray-dried as described above.

Confocal Laser Scanning Microscopy

Rhodamine-conjugated Fab1 was used as a probe for visualizing spray-dried particles within the PLGA–triacetin formulation. The rhodamine–Fab1-loaded formulations were observed using a Zeiss LSM 510 confocal microscope (Thornwood, New York) and the images were obtained after excitation at 480 nm and emission at 520 nm.

Rheology of PLGA–Triacetin Formulations

The flow curves of PLGA–triacetin formulations were measured using stainless steel parallel plate geometry on an ARG2 rheometer (TA Instruments, New Castle, Delaware). Approximately 200 μL of the formulation were placed on the rheometer and the gap height was set to 500 μm; excess formulation was carefully pipetted out. Sample was equilibrated at 25°C and viscosity was measured while simultaneously changing the shear rate ($d\gamma/dt$) from 10 to 1000 s^{-1}. The viscosity in the plateau region of the flow curve at low shear rate (10 s^{-1}) was considered as the zero-shear viscosity (η_0).

Atomic Force Microscopy

A MultiMode Atomic Force Microscope (Nanoscope V controller; Bruker, Santa Barbara, California) was used to measure the nano/micromechanical properties of the PLGA–triacetin depot *in situ*. Tapping mode atomic force microscopy (AFM) was used to image depot surface topography by minimizing the imaging force. The depot surface roughness at each time point was calculated from root-mean squared roughness of an image scan of 4×4 μm^2. The elastic modulus (E) of the depot surface layer was measured by indenting the surface with a colloidal probe with a 10-μm diameter borosilicate glass microsphere. The approach force curves were fitted to a Hertz model describing the indentation of semi-infinite elastic solid by a rigid sphere. The equation is presented in Figure 7a where F is the force, E is the Young's modulus, R is the sphere radius, δ is the indentation depth, and υ is the Poisson ratio.

In Vitro Fab1 Release

For *in vitro* release studies, approximately 50 μL of the PLGA–triacetin formulation (in triplicate) were injected through a 27G needle to the bottom of 3 mL PBS (pH 7.4) consisting of 0.01% (w/v) PS 20 and 0.02% (w/v) sodium azide in a 7-mL glass vial. The vials were capped, sealed, and placed in a warm room (at 37°C) under static conditions. *In vitro* drug release was conducted for up to 77 days and sampling was performed once every week. At each weekly time point, 2 mL of the release buffer was replaced with fresh buffer and the amount of Fab1 released was quantified using a modified Bradford assay described below. The cumulative drug release and standard deviation of the triplicate samples were calculated at each time point. Release testing under agitation was performed on a rocker platform shaker (BellCo, Vineland, New Jersey) set at 3 (equivalent to 4 oscillations per minute).

Bradford Assay

In each well of a 96-well plate, 150 μL of sample or standard in release buffer was added and 150 μL of Coomassie Plus™ Protein Assay Reagent (Thermo Scientific) was added. The plates were then read at 450 and 595 nm using a Biotek Synergy H4 Hybrid microplate reader (Winooski, Vermont). The concentration range for the standard curve was 1–50 μg/mL.

Fab1 Extraction from PLGA–Triacetin Depots

The depots were carefully separated from the aqueous phase and dried under vacuum for at least a week to completely remove the moisture. A mixture of THF and DCM (5 mL, 50:50 by volume) was added to the dried depot to selectively dissolve the polymer. The precipitated Fab1 was recovered after centrifugation at 931xg for 5 min. The recovered Fab1 was resuspended in 5 mL THF, vortexed, and centrifuged to remove any residual polymer. The wash solutions were collected together and preserved for polymer molecular weight analysis. Finally, the recovered Fab1 particles were washed in 3 mL petroleum ether, vortexed, and separated by centrifugation. The recovered Fab1 was dried by nitrogen purging and preserved under vacuum at ambient temperature until the analysis.

Size-Exclusion Chromatography

Size-exclusion chromatography (SEC) was performed using an Agilent 1200 series HPLC system on a TOSOH TSK-Gel Super SW2000 (4.6×300 mm^2) column and equipped with a diode array detector (DAD). Samples were eluted at 25°C in isocratic mode with 0.20 M K_3PO_4, 0.25 M KCl, pH 6.2 as the mobile phase at a flow rate of 0.2 mL/min. Prior to analysis, samples were diluted to approximately 1.0 mg/mL in PBS and 100 μL sample was injected. The total run time was 30 min and absorbance at 280 nm was used for detection. The SEC peaks were divided into monomer, high molecular weight species, and fragments. The percent peak area was calculated by dividing the peak area of each group at each time point to the total peak area.

Ion-Exchange Chromatography

Ion-exchange chromatography (IEC) was performed using an Agilent 1200 series HPLC system on two Dionex (Sunnyvale, California) ProPac® SAX-10 (2×250 mm^2) strong anion-exchange columns connected in series and equipped with a DAD. Mobile phase A and B (2.4 mM Tris, 1.5 mM imidazole, and 11.1 mM piperazine) were at pH 3.55 and 11.00, respectively. A linear gradient starting from 0% solvent A at 2 min to 100% solvent A at 64 min was employed to separate Fab charge variants in a total of approximately 100 min run time. Prior to analysis, samples were diluted to approximately 0.05 mg/mL in PBS, and 100 μL sample was injected. The absorbance at 280 nm was used for detection. The IEC peaks were divided into main peak, acidic peaks, and basic peaks. The percent peak area was calculated by diving each peak area to the total peak area.

 DOI 10.1002/jps.24546

Gel Permeation Chromatography

Gel permeation chromatography (GPC) analysis was performed using an Agilent 1200 series HPLC system equipped with a RI detector and a Zorbax PSM bimodal column (6.2 × 250 mm^2, 5 μm particle size). THF as a mobile phase was used at a flow rate of 1.0 mL/min. The column was calibrated using Polystyrene standards in the molecular weight range of 5×10^2–5×10^6 Da. PLGA number-average molecular weight (M_n) and its distribution (PDI) were estimated from the polystyrene standard calibration data. Except for the polymers recovered from depots, all other polymer samples were dissolved in THF at 1 mg/mL concentration. For the polymers recovered from depots (see Fab1 extraction procedure from PLGA–triacetin depots), the samples were diluted in THF prior to analysis.

Antigen-Binding Capacity by Surface Plasmon Resonance

Antigen binding capacity was measured on a Biacore T200 surface plasmon resonance system (Biacore T200; Pharmacia, Piscataway, New Jersey). Antigen of Fab1 was covalently immobilized onto the carboxymethylated dextran sensor chip (CM5) using amine coupling kit (GE Healthcare). First, the dextran sensor chip was activated by 1:1 (v/v) mixture of 0.4 M 1-ethyl-3-(3-dimethylaminoproply)-carbodiimide (EDC) and 0.1 M NHS at 10 μL/min for 420 s. The antigen was then immobilized onto the EDC–NHS-activated surface by flowing through 100 μg/mL antigen (diluted in 10 mM sodium acetate at pH 5) at 10 μL/min for 180 s. The excess reactive groups were then deactivated with 1 M ethanolamine–HCl for 420 s. The amount of antigen immobilized was in the range of 2000–3000 resonance units (RU). The binding of Fab to its antigen was determined by monitoring the change in the RU before and after injection for 180 s. The sensor chip was regenerated with 10 mM glycine–HCl, pH 2.1 at 30 μL/min for 30 s. All binding assays were performed at room temperature in HEPES buffer [0.01 M HEPES, 0.15 M NaCl, 0.005% (v/v) surfactant P20, pH 7.4]. The antigen-binding concentration was calculated from a standard calibration curve (0.158–5 μg/mL) using a four-parameter fit. The ratio of this concentration to the total protein concentration determined by Bradford assay or UV absorbance measurement gives the antigen-binding capacity. The antigen-binding capacity at each time point normalized the antigen-binding capacity at t_0.

Fab pH Stability

To evaluate the pH-dependent stability, Fab1 was formulated at 5 mg/mL in various pH buffers: 10 mM phosphate (pH 2.2, 3.9, 7.2), 10 mM acetate (pH 4.7), and 10 mM histidine–HCl (pH 6) with 10 mg/mL trehalose and 0.02% (w/w) PS20. The samples in different buffers were taken in 7 mL glass vials. The vials were capped and sealed with parafilm and placed in the warm room (37°C) stability testing. The samples were collected at different time points and the stability was evaluated with surface plasmon resonance, IEC, and SEC methods described above.

Water Uptake Measurement

At selected time points, the release buffer was removed from the PLGA–triacetin depots (in triplicate) and the wet depot mass (m_w) was measured. The depots were then dried under vacuum at ambient temperature for over 2 weeks and then the dry depot masses (m_d) were measured. The percent water content was calculated from the difference in wet and dry depot masses divided by wet mass [$W = (m_w - m_d)/m_w$)].

RESULTS

Characterization of Spray-Dried Fab1

An aqueous Fab1 solution containing trehalose and PS20 in pH 5.5 histidine–HCl buffer was spray-dried to yield a solid drug formulation. Trehalose and PS20 were included in the formulation as excipients for maintaining Fab1 stability during the drying operation and long-term residence in solid state. A pH of 5.5 was selected as optimal based on the pH-dependent degradation profile of Fab1 in aqueous formulations (will be discussed later). To maintain drug stability in the solid state, the mass ratio of trehalose to protein in the formulation was maintained at 1.0.

The spray-drying process yielded a free-flowing and white powder containing approximately 42% Fab1 (UV spectrophotometric assay) and 5.5% moisture (KF method); the remainder of the spray-dried powder was presumably composed of trehalose and histidine–HCl buffer (excipients). SEM images (Fig. 1a) of the spray-dried powder showed that the particles were micron-sized and possessed a smooth topography that was characterized by large surface dimples. Laser diffraction measurement of particle size distribution indicated that 90% (D90) of the particles were within the range 5.70 (±0.42) μm (Fig. 1b). Although laser diffraction data provide a measure of global average particle size based on volume distribution, the SEM images provide a direct visualization of the particle size and its distribution (Fig. 1a).

Fab1 quality before and after the drying process was assessed using SEC and IEC methods. The SEC of Fab1 samples before and after drying (Fig. 1c) showed a dominant monomer peak (retention time: 15.5 min) with a relative peak area of 99.4% and 99.5%, respectively. Similarly, the IEC main peak area (retention time: 43.7 min) for the samples (Fig. 1d) before and after the spray-drying process was 95.4% and 94.5%, respectively. The SEC and IEC together confirm that the spray-drying process did not adversely impact the quality of Fab1.

Formulation Preparations and Characterization

Figure 2a outlines the formulation preparation procedure. Spray-dried Fab1 powder was added to a clear and colorless PLGA–triacetin solution and the contents were mixed to form a viscous and opalescent suspension that was readily injectable through a 27G needle. When the formulation was injected into aqueous PBS buffer, it formed a distinct phase that was physically stable. There was no perceptible evidence for aqueous and nonaqueous phase mixing (Fig. 2c). To visualize Fab1 particle distribution within PLGA–triacetin solution, rhodamine-conjugated Fab1 was spray-dried and encapsulated within the PLGA–triacetin solution. Fluorescence microscopy image (Fig. 2d) shows that the spray-dried particles were homogeneously distributed within the depot and the particles mostly existed as discrete micron-sized entities, without any evidence for particle phase separation.

To assess the impact of polymer molecular weight on formulation physical properties and *in vitro* drug release profiles, three PLGA polymers (Fig. 2b) that differed only in their molecular weights but possessing identical end group (alkyl ester) and lactide content (75%) were selected. Table 2 lists the M_n

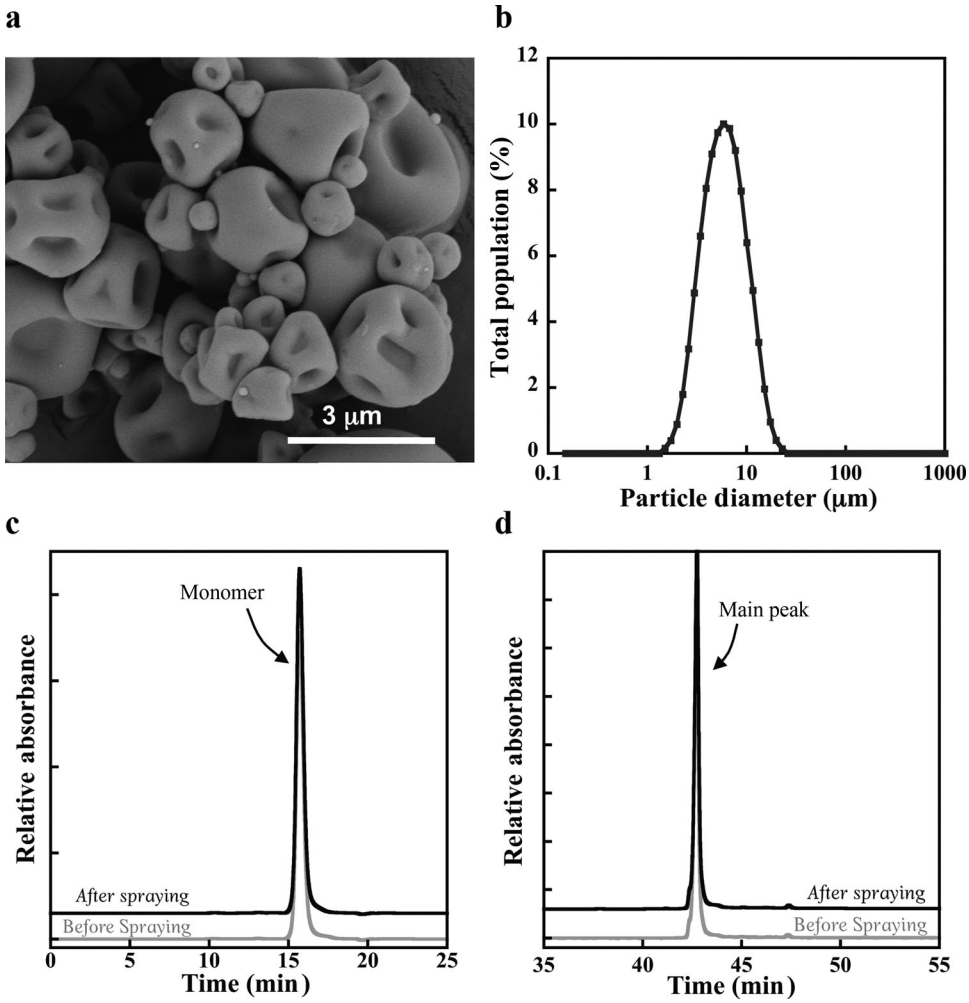

Figure 1. Characterization of spray-dried Fab1. (a) SEM micrograph of spray-dried Fab1 particles. (b) Laser scattering measurement of Fab1 volume-averaged particle size distribution. (c) SEC of Fab1 before and after spray-drying process. (d) IEC of Fab1 before and after spray-drying process.

and glass transition temperature (T_g) of the three PLGA polymers selected for this study.

Rotational rheology was used to assess the formulation flow properties, both with and without Fab1. Within the shear rates investigated, PLGA–triacetin solutions devoid of drug exhibited Newtonian flow behavior (Fig. S1A). η_0 increased either with increasing polymer concentration or polymer molecular weight (Fig. 2e). For example, the viscosity of pure triacetin was 0.05 Pa s and increased to 1 and 10 Pa s for 20% PLGA-10k and 20% PLGA-56k solutions, respectively. Likewise, the viscosity of Fab1-loaded formulation also increased with increasing Fab1 concentration (Fig. 2f). Although no clear yield point was observed in the flow curves (Fig. S1B) of Fab1-loaded suspensions, the viscosities at low and high shear rates deviate at higher drug loadings.

Fab1 Release from PLGA–Triacetin Depots

Five formulations (Table 1) were designed to systematically probe the effects of polymer concentration and polymer molecular weight on *in vitro* Fab1 release profiles. In the first formulation set (Table 1a), Fab1 concentration was kept constant and the polymer concentration was varied from 7.5% to 12.5% (w/w). In the second set (Table 1b), the polymer and Fab1 concentrations were kept constant but the polymer molecular weight was varied from 10 to 56 kg/mol.

Figure 3 shows the cumulative amount of Fab1 released with time for the first set of formulations that differed only in polymer concentration. The release profile shows multiple phases but two predominant phases can be noted: an initial slow release phase that lasted for about 21 days and a subsequent rapid release phase that lasted until day 77. The inset in Figure 3 shows that the initial burst release is inversely related to PLGA concentration in the formulation. Although 8% Fab1 was released from the formulation containing 7.5% polymer after 21 days, less than 1% Fab1 was released from the formulation containing 12.5% polymer during the same period. Interestingly, regardless of PLGA concentration, the drug release profile of all three formulations showed a fast-release phase approximately from day 21 onwards. Even though the overall release profiles were similar, a clear trend relating the amount of drug released and the polymer concentration can be noted. Generally, increasing the polymer concentration tends to decrease the drug release rate.

Figure 4a shows the time-dependent changes in polymer gel permeation chromatograms for the formulation containing

 DOI 10.1002/jps.24546

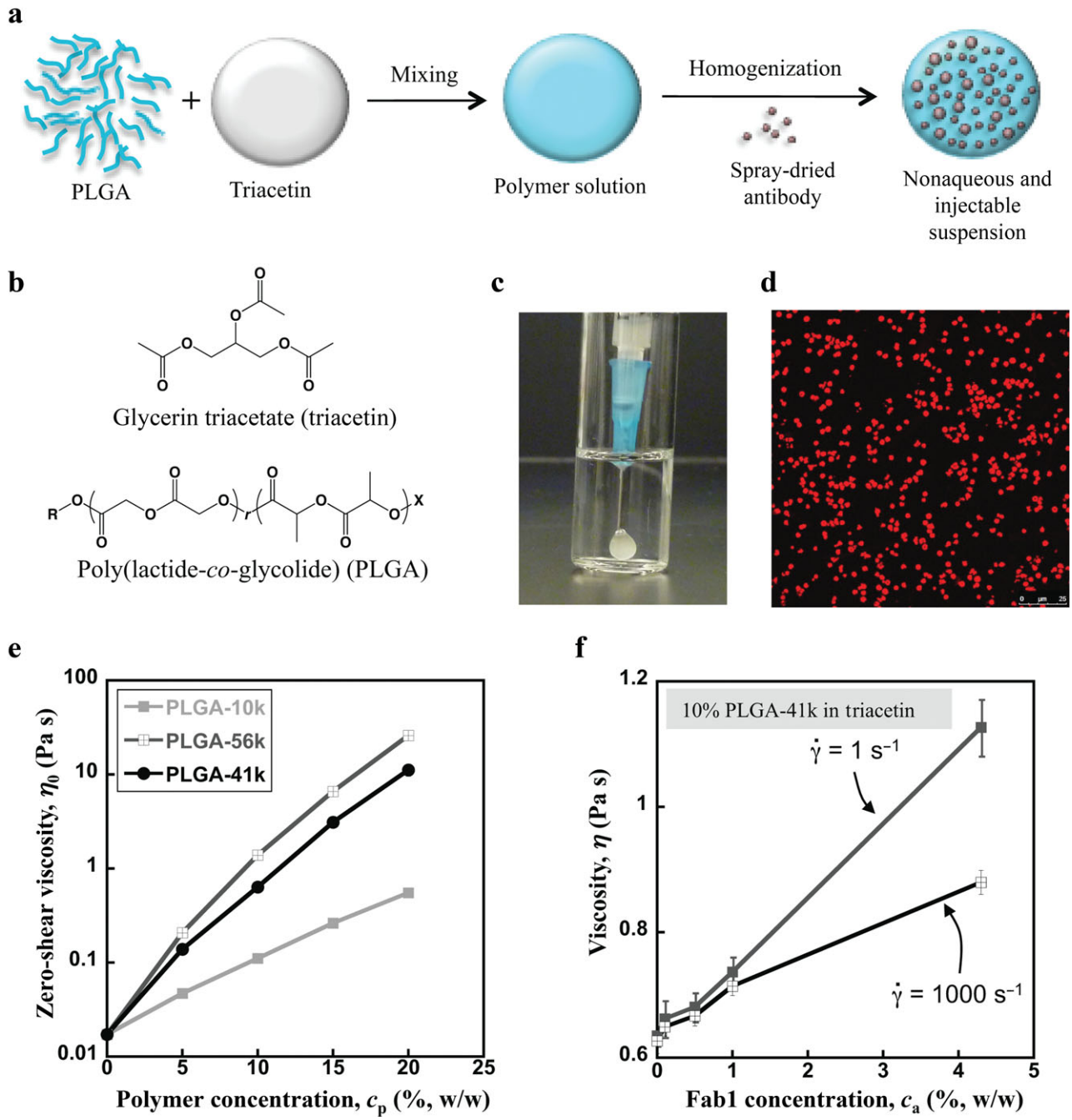

Figure 2. Preparation and characterization of PLGA–triacetin depot formulation. (a) Spray-dried Fab1 formulation is added to PLGA–triacetin solution and homogenized to form a nonaqueous and injectable suspension. (b) Molecular structure of triacetin and PLGA. (c). Injectability of Fab1-loaded PLGA-triacetin formulation through a 27G needle and depot formation in PBS. (d) Fluorescence microscopy image of rhodamine–Fab1-loaded formulation. (e) Change in the zero-shear viscosity (η_0) of PLGA–triacetin solution as a function of polymer concentration for three PLGA polymers. (f) Viscosity of Fab1-loaded PLGA–triacetin formulation containing 10% PLGA-41k at low and high shear rates.

Table 2. Polymer Characterization Details

Polymer	Lactide–Glycolide	MW (M_n, kg/mol)	PDI (M_w/M_n)	Glass Transition Temperature (T_g, °C)
PLGA-10k	75:25	10.0	1.9	35
PLGA-41k	75:25	41.3	1.5	46
PLGA-56k	75:25	56.7	1.5	46

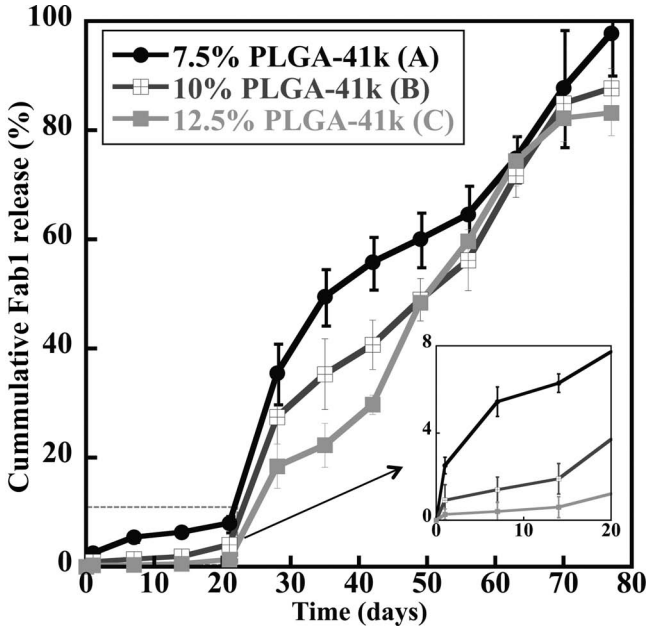

Figure 3. Effect of polymer concentration on Fab1 release. Cumulative Fab1 release from PLGA–triacetin depots containing varying amounts of PLGA-41k. Inset shows magnification of release profile during the first 20 days.

1.5% Fab1 in 10% PLGA-41k solution. M_n gradually decreased from 40 kg/mol to less than 5 kg/mol after 70 days in PBS (Fig. 4b). GPC show that the decrease in polymer molecular weight was also accompanied by a broadening of the molecular weight distribution (Fig. 4a).

Scanning electron microscopy imaging was used to assess the changes in depot microstructure. Figure 5 shows the SEM images collected during different stages of release for the formulation containing 10% PLGA and 1.5% Fab1. The depot surface appeared smooth on days 1 and 14 but the cross-section was highly porous. The day 14 sample did have surface pores but they were limited to a small region of the depot surface (Fig. S2). A closer look into these pores reveals that they are interconnected and seem to penetrate deep into the depot. On days 42 and 77, the depot surface appeared deformed, clearly indicating that the depot had undergone mass erosion.

Gravimetric measurement of depot mass before and after drying indicates that distinct mass changes occur after day 21. Figure 6a shows that after day 21, the wet depot mass increased with time, whereas the dry depot mass decreased with time. The difference between wet and dry depot masses is equivalent to the water taken up minus the outflow of triacetin from the depot. After initial increase, the water content (Fig. 6b) leveled off at 76% until day 21 and gradually increased to 96% on day 79.

To assess how the temporal change in depot mass influences its mechanical properties, AFM was used to probe the *in situ* stiffness of the depot surface and surface roughness. Figure 7a depicts the model employed for estimating the depot stiffness *in situ*. A 10-μm colloidal probe was attached to the AFM tip and the microelasticity of the depot surface was measured by indentation. The Young's modulus (E) or the stiffness of the depot surface was estimated by fitting the force and indentation curve to a Hertz model (Fig. 7a, equation). Measured in this manner, the surface stiffness on days 1 and 13 are around 5 MPa and increased to 200–300 MPa on days 23 and 28. *In situ* AFM imaging (Fig. 7c) reveals the microscale and nanoscale structural details of the depot surface. An increase in surface roughness (R_q) from 0.8 to 1.7 nm over 21 days was observed.

Figure 8a compares the effect of changing polymer molecular weight on Fab 1 release at identical polymer and Fab1 concentrations. Interestingly, the initial lag phase observed in the drug release profile from the formulations prepared using either PLGA-41k or PLGA-56k polymer was absent in the formulation prepared using PLGA-10k polymer. From the formulation containing PLGA-10k polymer, more than 80% of the total Fab1 loaded was released within the first 7 days and the remaining 20% was released slowly between days 7 and 77. Whereas from the formulation containing PLGA-41k polymer, less than 5% of drug was released during the first 21 days and 78% of total loaded drug was released between days 21 and 77. Between the PLGA-41k and PLGA-56k formulations, however, no appreciable difference in drug release profile was observed.

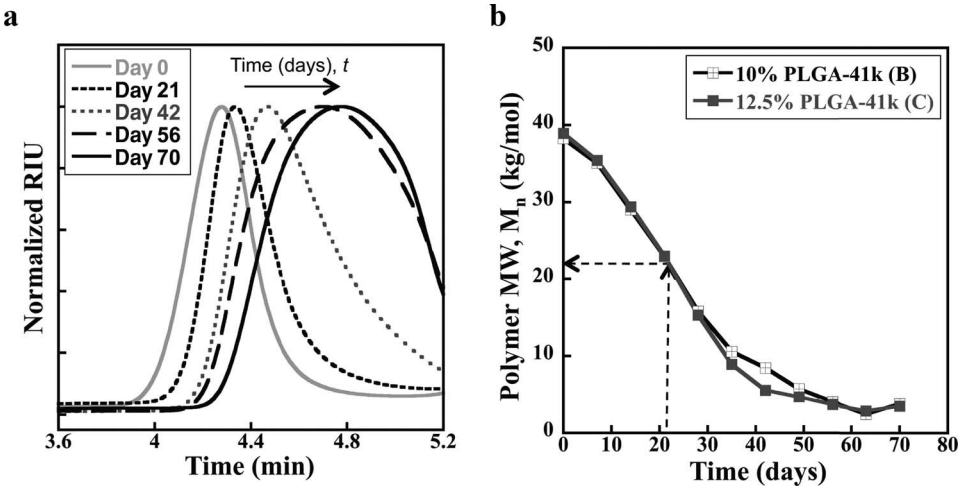

Figure 4. Polymer degradation and changes in MW (a) GPC chromatograms showing changes in PLGA molecular weight distribution. (b) Change in the number average molecular weight (M_n) of PLGA with time.

 DOI 10.1002/jps.24546

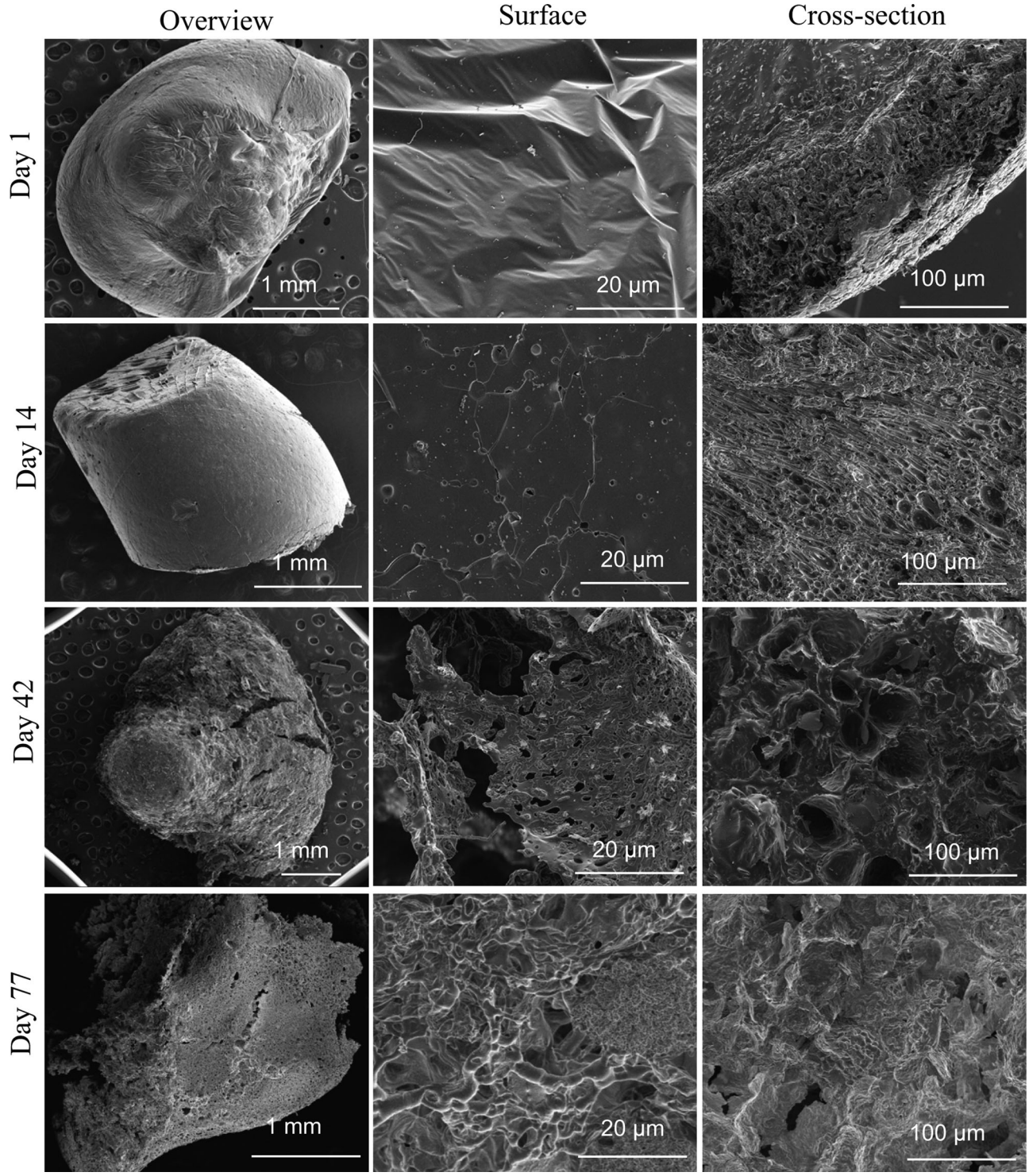

Figure 5. Changes in depot microstructure. SEM images of depot surface and cross-section during different stages of *in vitro* release.

Measurement of polymer molecular weight during *in vitro* release suggests that it decreased monotonically with time for all three formulations (Fig. 8b).

Fab Stability in PLGA–Triacetin Depots

The temporal changes in the physical and chemical stability of Fab1 during *in vitro* release were assessed after its recovery from depots at different stages during *in vitro* release. A solvent mixture composed of THF and DCM was used to selectively dissolve the polymer and the precipitated drug was recovered in solid form after vacuum drying. That the extraction procedure employed does not affect Fab1 stability was confirmed by comparing the SEC (Fig. S3A) and IEC (Fig. S3B) chromatograms and CD spectra (Fig. S4) of Fab1 after extraction from the depot with that of the Fab1 sample obtained immediately after spray drying. Figure 9a shows the change in Fab1 main peak

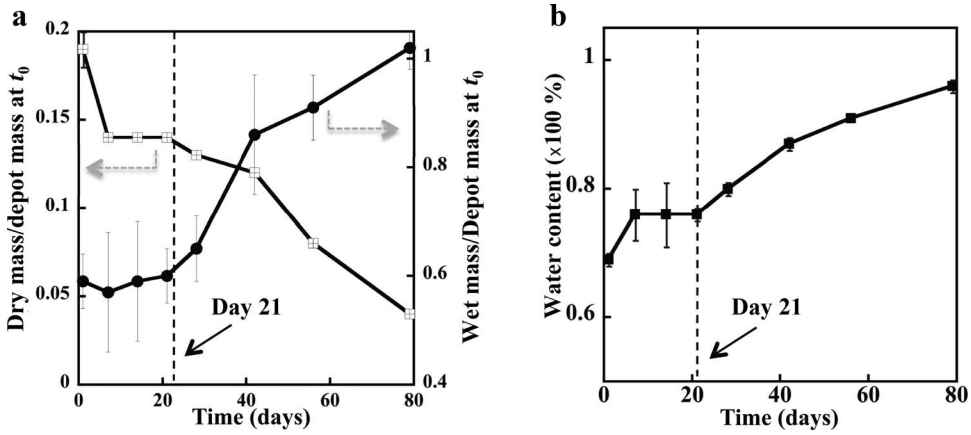

Figure 6. Temporal changes in wet and dry depot mass. (a) The changes in wet (m_w) and dry (m_d) masses normalized to the depot mass at t_0 are shown with time. (b) The amount of water [$W = (m_w - m_d)/m_w$)] taken up by the depot is shown with time. Note the distinct changes from day 21 onwards in both plots.

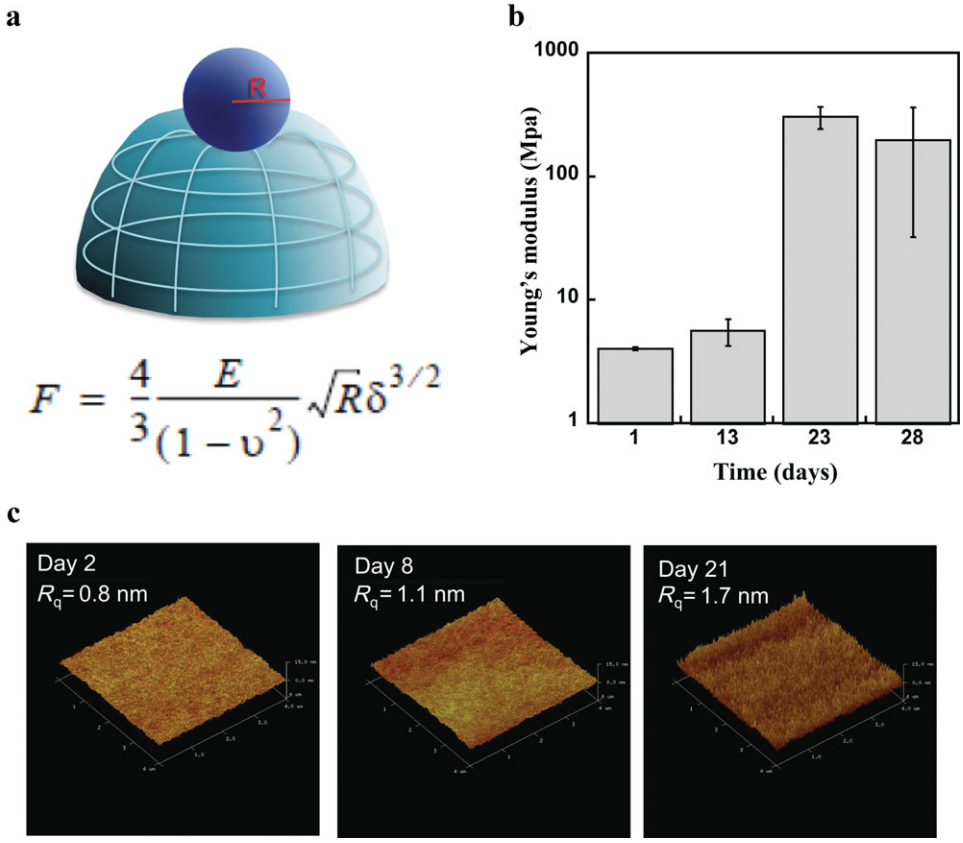

Figure 7. *In situ* measurement of depot stiffness and surface roughness. (a) Hertz model depicting the measurement of depot surface stiffness using a colloidal probe attached to AFM tip. F is the force, E is the Young's modulus, R is the sphere radius, d is the indentation depth, and u is the Poisson ratio. (b) *In situ* Young's modulus of the depot surface at different stages of release. (c) *In situ* images of depot surface at different stages of release. The roughness value was calculated from the AFM images.

(measured from IEC) and monomer content (measured from SEC) after recovery from depots at different stages of release. Although the SEC monomer content reduced slowly from 99.5% on day 0 to 97.0% on day 77, the IEC main peak reduced at a much faster rate; it dropped from 97.0% on day 0 to 45.0% on day 77. The IEC method employed a strong anion-exchange column for separation using a pH gradient elution method. The acidic and basic peaks, therefore, are generated to the right and left of the main peak (44.6 min), respectively. Comparison of IEC chromatograms (Fig. 9b) suggests that both acidic and basic peaks increased with time during residence within the depot.

To elucidate the pH effects on Fab1 chemical degradation and correlate with its degradation within the depot, Fab1 chemical stability (at 5 mg/mL) was assessed separately in five different aqueous buffers ranging from pH 2.2 to 7.4. Figure 9c shows

 DOI 10.1002/jps.24546

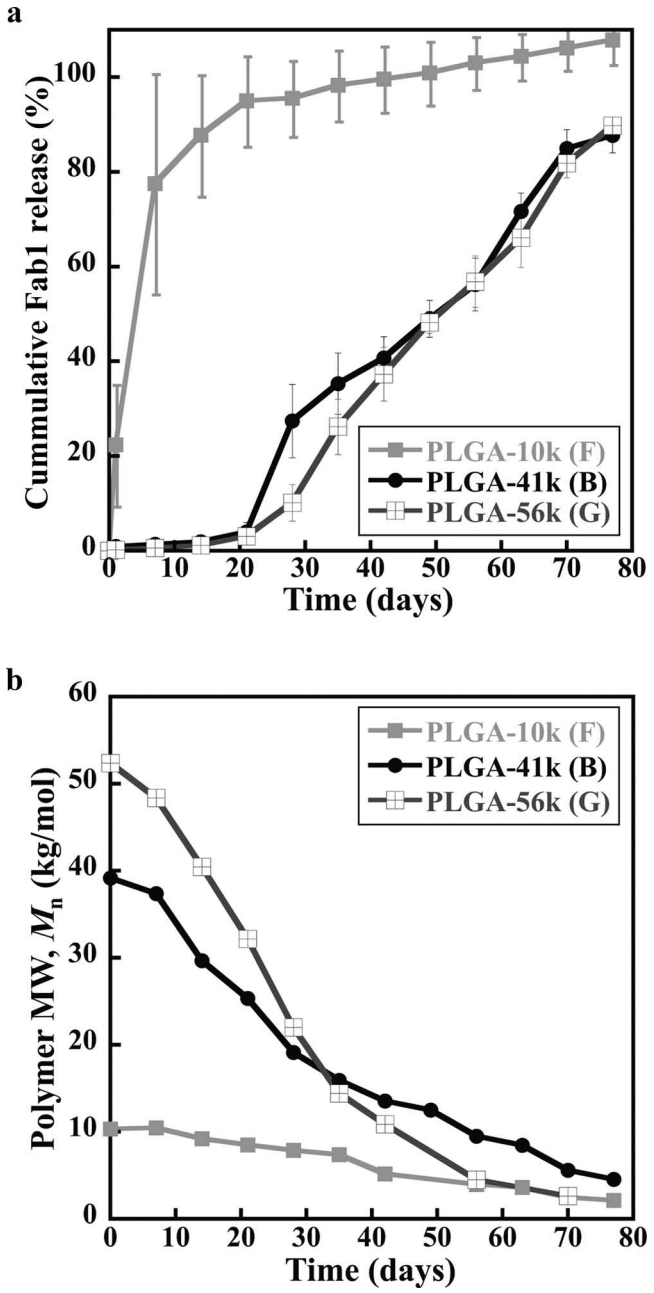

Figure 8. Effect of polymer MW on *in vitro* release and degradation. (a) Cumulative Fab1 release from PLGA–triacetin depots containing identical PLGA concentrations but different molecular weights. (b) Change in PLGA number average molecular weight, M_n, with time during *in vitro* release.

all five IEC traces after 56 days incubation at 37°C in aqueous buffer. It is clear that both deamidation (acidic peaks) and succinimide intermediate product (basic peaks) formation reactions were more pronounced in pH 2.2, 3.9, and 7.4 solutions than in pH 4.7 and 6.0 solutions. Not surprisingly, chemical degradation at pH 2.2 was greater than at any other pH investigated. After 56 days at 37°C, the main peak reduction was 56.5% and 6.1% in pH 2.2 and pH 6 buffers, respectively. Interestingly, the rate of main peak loss during its residence within depot is comparable with the rate of main peak loss in aqueous pH 7.4 buffer (Fig. S5). However, a close scrutiny of IEC chromatograms in Figures 9b and 9c indicates that they are slightly different. In the Fab1 sample recovered from the depot, the dominant acidic peak and basic peaks elute at 44.4 and 45.5 min, respectively, whereas the pH-dependent degradation peaks elute at 43.0 and 45.6 min.

To assess how the chemical degradation in Fab1 affects its activity, antigen-binding assays were performed on all pH-stressed samples as well as on Fab1 recovered from PLGA–triacetin depot after incubation at 37°C over time. Figure 9d shows the antigen-binding capacity normalized to t_0 sample over time. The rate of decrease in antigen-binding capacity of the extracted Fab1 follows the same rate as in pH 7.2 buffer. The decrease in antigen binding is significantly less than the decrease in IEC main peak (i.e., chemical degradation), thus suggesting that some chemical degradation may not directly contribute to loss in binding capacity.

DISCUSSION

Herein, we have demonstrated that sustained delivery of a large hydrophilic molecule such as an antibody fragment can be achieved from a polymer–solvent-based delivery system. We have further showed that changing the polymer molecular weight or its concentration can modify the drug release kinetics. Importantly, the drug was functionally active during its long-term residence within the depot and throughout the different stages of the preparation process. Inclusion of trehalose in the formulation helps to maintain Fab1 stability in the native state. The presence of this trehalose is known to stabilize proteins against aggregation in the solid state.[28,29] Despite significant chemical changes, as revealed by IEC, the fragment antibody retains a high level of antigen-binding capacity (>80% relative to starting material) after 77 days. The relationship between the extent of chemical degradation and antigen-binding capacity however is amino acid sequence and structure dependent.

The occurrence of acidic microenvironments within PLGA-based drug delivery systems because of the generation and accumulation of low molecular weight degradation products, lactic, and glycolic acids is a well-established phenomenon.[30–34] It is however unknown whether low pH conditions also prevail within the PLGA–triacetin depot. The actual pH that Fab1 encounters within the depot has not been empirically determined here but it appears that the antibody does not "experience" low pH condition normally present in PLGA-based systems. Environmental pH largely governs the chemical stability of proteins. A comparison of pH and time-dependent chemical degradation of Fab 1 in aqueous buffers with the time-dependent chemical degradation during its residence within the depot provides a rough idea of the pH prevailing within the depot or at least the pH "experienced" by the Fab. Interestingly, the rate of main peak loss in the Fab1 sample recovered from the depot is similar to the rate of main peak loss in the Fab1 sample that was incubated in aqueous buffer at pH 7.4 (Fig. S5). This implies that the pH within the depot does not reduce to lower values but is perhaps closer to the pH of the exterior medium. The drug in spray-dried form is more resistant to degradation or the porous interiors within the depot permits rapid exchange of buffer components and polymer degradation products, thus alleviating the accumulation of protonated lactic and glycolic acids within the depot. The evaluation of long-term drug

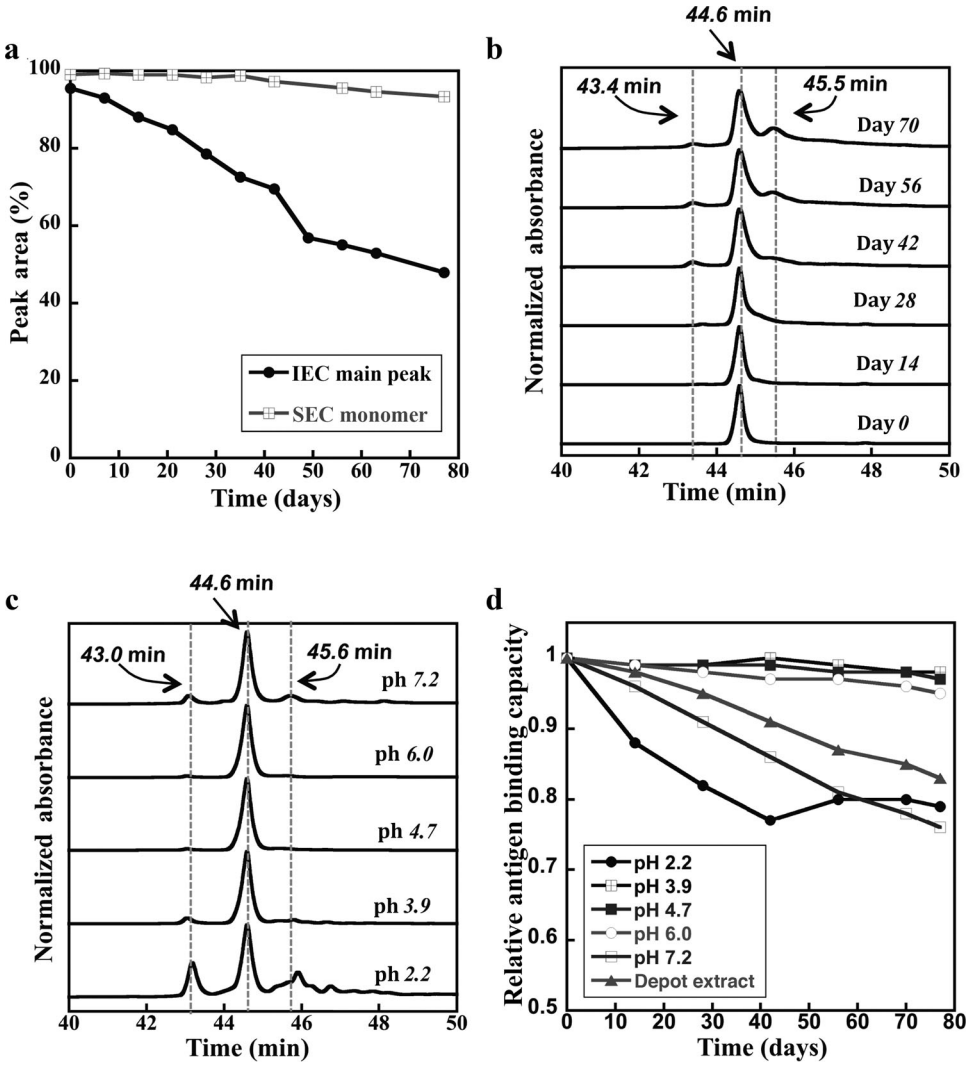

Figure 9. Characterization of Fab1 stability. (a) Change in Fab1 IEC and SEC main peak and monomer peak areas. Samples were analyzed after recovery from depots during different stages of *in vitro* release. (b) Fab1 IEC chromatograms during different stages of *in vitro* release. (c) Fab1 IEC chromatograms after incubation in various pH buffers for 56 days at 37°C. Peak eluting at 44.6 min in c and d corresponds to main peak (undegraded Fab1). (d) Antigen-binding capacity of Fab1 after incubation in various buffers at 37°C and after recovery from depot.

stability at pH 7.4 and 37°C can therefore be considered as a good indicator of drug stability within the PLGA–triacetin depot.

The storage stability of Fab1 in triacetin and PLGA–triacetin solution, but in the absence of aqueous release buffer, was also investigated separately at 37°C. Even after 3 months at 37°C, the monomer content and main peak was 98.2% (reduced by 0.1%) and 97.7% (reduced by 0.4%), respectively (Fig. S6). This confirms that both triacetin and PLGA–triacetin solution under anhydrous conditions do not impact the stability of Fab1. The spray-dried powder is inert in triacetin and the protein exists in solid state in the absence of water. During *in vitro* release however, water transfer into the depot followed by polymer degradation contributes to Fab1 degradation.

The mechanism of drug release is consistent with the model initially proposed by McHugh[35,36] and recently reviewed by Thakur et al.[37] and Parent et al.[38] The drug release mechanism is depicted in Figure 10a. Figure 10b shows the components that are transferred across the interface between the depot and aqueous exterior. The lag phase observed in Figure 2 can be attributed to the formation of a morphologically smooth surface barrier (termed "skin layer" or "membrane") at the interface between the organic depot and the aqueous release medium. "Membrane" formation is the result of the aqueous and organic phase demixing (phase inversion) resulting in polymer precipitation first at the interface to form a "membrane." The surface "membrane" presumably grows inwards as solvent efflux continues and the depot eventually becomes a solid while physically entrapping the spray-dried drug within the solidified hydrophobic polymer matrix. The lack of drug release during initial stages of release supports the observation that the surface "membrane" is diffusion limiting. This hypothesis is also corroborated by previous observations that rapidly exchanging hydrophilic solvents such as DMSO and NMP facilitate the burst drug release, and slowly exchanging solvents such as triacetin and ethylbenzoate are known to shut down drug release.[16,39] The observation of a smooth depot surface in the SEM images (Fig. 5) on days 1 and 14 and the occurrence

 DOI 10.1002/jps.24546

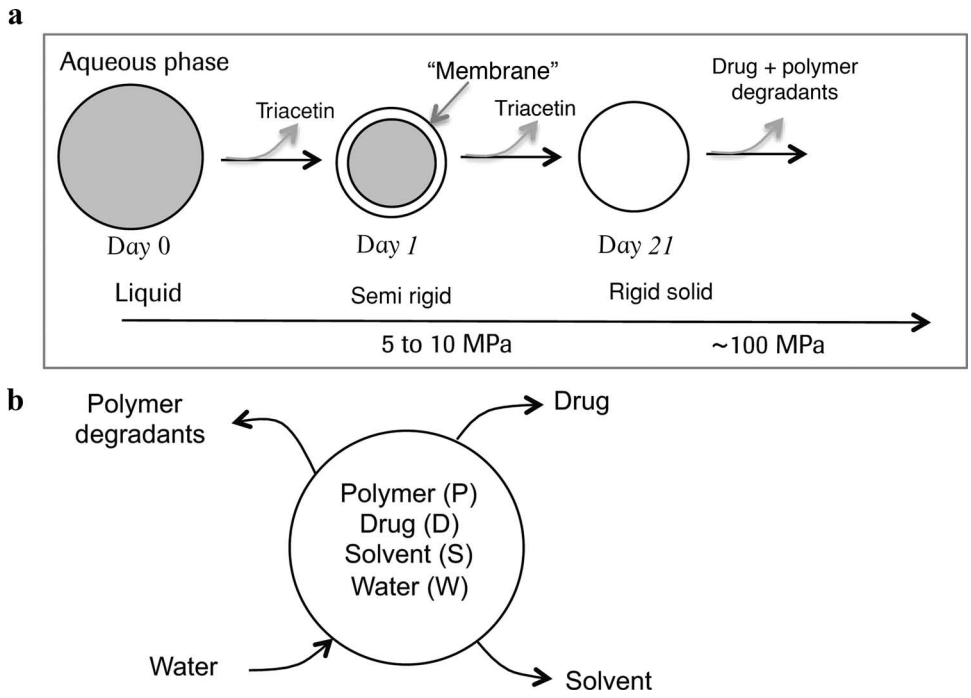

Figure 10. Depot formation and drug release mechanism. (a) A diffusion-limiting 'membrane' is formed on day 1 at the depot surface because of solvent efflux and polymer precipitation. The membrane grows inwards slowly with time to form a solid material by day 21. From day 21 onwards, water uptake increases and facilitates drug release and depot erosion. (b) Mass transport of components into and out of depot during drug release.

of a lag phase till day 21 (Fig. 3) together affirm the formation of a diffusion-limiting surface membrane in the current study.

Temporal changes in the wet and dry depot masses (Figs. 6a and 7b) also parallel the drug release profile. The depot mass, measured gravimetrically, increases on day 1 because of water uptake but it ceases until day 21 before increasing again. This clearly suggests that the surface membrane is impervious to the transport of water and drug molecules across the interface during the lag phase. It is likely that residual triacetin retained in the depot maintains a fluidic interior until its exit is fully complete, but the mass change because of triacetin efflux alone may not be discernable in a gravimetric measurement. The depot solidification process because of triacetin efflux and inward membrane growth is likely to be completed before the end of the lag phase. The fact that only 8% of Fab1 was released on day 21 (Fig. 3) suggests that most of the drug is buried within the solid polymer phase and therefore is not readily available for release. After the completion of depot solidification process, water uptake followed by material erosion facilitates the slow drug efflux by diffusion. Consequently, the drug release profile after the lag phase approximates to the drug release from a solid degradable matrix (Fig. 3).

Atomic force microscopy provides unique insights in to the *in situ* depot properties. Force indentation using a colloidal probe enables the estimation of the depot surface stiffness and imaging in scanning mode provides a direct measure of the surface roughness. The *in situ* stiffness measurement shows that a fluid that is initially injectable via a 27G needle first transitions to a semirigid gelatin-like material (Young's modulus, $E = 5$ MPa) in aqueous phase and then to a rigid solid ($E = 200$–300 MPa) after approximately 21 days (Fig. 7b). The increase in surface rigidity over time follows the observed depot solidification process indicated earlier. The surface roughness (R_q) measured from AFM images provides an indication of the surface morphology at the micro/nanometer length scale. An increase in R_q (Fig. 7c) from 0.8 nm on day 1 to 1.7 nm on day 15 reveals that the depot surface gradually becomes rough over time. AFM, however, can only probe the surface properties and does not reveal the physical state of the depot interior.

The injectability of a sustained-release formulation is a major functional advantage in drug delivery. The determination of injectability parameters is important but it was not our primary goal here because injectability is dependent on a number of factors, including syringe and needle geometry, delivery volume, injection duration, and the nature of target site. Nonetheless, it was necessary to understand how changes in polymer concentration, polymer molecular weight, and drug-loading impact formulation viscosity. For the current study, the viscosity information was utilized for designing formulations such that the final formulation viscosity was within the range 1.0 ± 0.3 Pa s. Formulation viscosity can influence the initial drug release rate—immediately after administration when the depot is still fluidic. Although the high shear rate ($\gamma = 1000\ s^{-1}$) viscosity determines syringe ability, the low shear rate viscosity dictates particle movement within the depot and can impact the diffusion-controlled drug release. The formulation viscosity increased either with polymer molecular weight or its concentration. Consequently, Fab1 release rate on day 1 decreased with either increasing polymer concentration or molecular weight.

A comparison of polymer degradation and (Fig. 4b) drug release rates (Fig. 3) suggests no apparent correlation. Although the release profile had a clear inflection point on day 21, the polymer molecular weight decreased monotonically with time. At the end of slow drug release phase, that is, on day 21,

when only less than 8% of the total Fab1 loaded was released, the polymer molecular weight had already dropped to approximately 21 kg/mol. Comparison of Fab1 release profile (Fig. 8a) with the polymer degradation profile (Fig. 8b) may indicate that drug release is accelerated when the polymer MW falls approximately below 30 kg/mol but the physical state of the depot at any given time influences the drug release profile. Because the T_g of PLGA-10k polymer is 35°C, the depot prepared using this polymer always remains as a viscous fluid at 37°C even after all triacetin has been transferred to the aqueous phase. When Fab1 release was measured from this formulation at 5°C, the release profile had a slow release phase preceding the fast release phase (Fig. S7), clearly suggesting that the polymer physical state, governed by its MW and T_g, can greatly influence the drug release profile. In contrast, the T_g of PLGA-41k and PLGA-56k polymer is 46°C and both these formulations transition to a solid material at 37°C after triacetin transfer to aqueous phase is complete.

In addition to polymer concentration and molecular weight, drug loading can also impact the release duration. The investigation of the effect of drug loading on release is currently ongoing. It is however expected that increasing the drug loading will cause an increase the drug release rate. When the drug loading goes beyond the percolation threshold, rapid drug release is expected. To achieve sustained drug release, it is therefore necessary to maintain the drug concentration below the percolation threshold. In the current study, sustained protein release for up to 80 days was accomplished at a drug loading of 1.5% by weight. With further optimization of drug loading, it may therefore be possible to extend the release duration beyond 80 days.

The *in vitro* release studies described here were conducted under static conditions. To test whether agitation impacts drug release profile, release testing was performed on a platform shaker with mild agitation (at 4 oscillations/min). Interestingly, agitation during release testing did not impact the drug release profile (Fig. S8). The extent of agitation required for release testing of sustained-release formulations is however dependent on the application for which the system has been designed. For intravitreal delivery, it is unclear how much agitation is relevant for *in vitro* release testing. Because of the formation of a semirigid depot with a diffusion-limiting surface "membrane," mild agitation has no impact on drug release profile.

CONCLUSIONS

We have presented the preparation, characterization, and *in vitro* performance of PLGA–tricetin formulations suitable for the long-term delivery of proteins. The effect of polymer concentration and its MW on the release of a fragment antibody has been investigated. Interestingly, we have found that when the polymer MW is large (>41k), a slow release phase is observed in the release profile. The results presented here indicate that both polymer concentration and molecular weight can be used to modulate the Fab release profile. The Fab stability was assessed at different stages during *in vitro* release. Comparison of pH-dependent changes in stability showed that the fragment antibody within PLGA–triacetin depot may not be exposed to low pH environments typically expected in other types of PLGA-based delivery systems such as microspheres or implants. The data presented here suggests that a combination of polymer MW and concentration can be utilized to modulate fragment antibody release profile over a period ranging from days to months. An understanding of the factors that control drug release will enable the design of formulations that can sustain drug release for longer duration. Importantly, the PLGA–triacetin formulation is injectable through a 27G needle. The results presented here show that PLGA–triacetin formulations could be promising systems for the long-term delivery of therapeutic proteins.

ACKNOWLEDGMENT

K.R. acknowledges Thierry Nivaggioli, Director, Drug Delivery Department, Genentech Inc., for thoughtful scientific discussions.

REFERENCES

1. Yasin MN, Svirskis D, Seyfoddin A, Rupenthal ID. 2014. Implants for drug delivery to the posterior segment of the eye: A focus on stimuli-responsive and tunable release systems. J Control Release 196:208–221.

2. Zhu GZ, Mallery SR, Schwendeman, SP. 2000. Stabilization of proteins encapsulated in injectable poly (lactide-co-glycolide). Nat Biotechnol 18:52–57.

3. Lee SS, Hughes P, Ross AD, Robinson MR. 2010. Biodegradable Implants for Sustained Drug Release in the Eye. Pharm Res 27:2043–2053.

4. Ghalanbor Z, Korber M, Bodmeier R. 2009. Improved Lysozyme Stability and Release Properties of Poly(lactide-co-glycolide) Implants Prepared by Hot-Melt Extrusion. Pharm Res 27:371–379.

5. Kempe S, Maeder K. 2012. In situ forming implants - an attractive formulation principle for parenteral depot formulations. J Control Release 161:668–679.

6. Dong WY, Korber M, Lopez Esguerra V, Bodmeier R. 2006. Stability of poly(D,L-lactide-co-glycolide) and leuprolide acetate in in-situ forming drug delivery systems. J Control Release 115:158–167.

7. Packhaeuser CB, Schnieders J, Oster CG, Kissel T. 2004. In situ forming parenteral drug delivery systems: an overview. Eur J Pharm Biopharm 58:445–455.

8. Koerber M, Bodmeier R. 2008. Development of an in situ forming PLGA drug delivery system I. Characterization of a non-aqueous protein precipitation. Eur J Pharm Sci 35:283.

9. Sinha VR, Trehan A. 2003. Biodegradable microspheres for protein delivery. J Control Release 90:261–280.

10. Ye M, Kim S, Park K. 2010. Issues in long-term protein delivery using biodegradable microparticles. J Control Release 146:241–260.

11. Kempe S, Metz H, Maeder K. 2008. Do in situ forming PLG/NMP implants behave similar in vitro and in vivo? A non-invasive and quantitative EPR investigation on the mechanisms of the implant formation process. J Control Release 130:220–225.

12. Wischke C, Zhang Y, Mittal S, Schwendeman SP. 2010. Development of PLGA-Based Injectable Delivery Systems For Hydrophobic Fenretinide. Pharm Res 27:2063–2074.

13. Schoenhammer K, Petersen H, Guethlein F, Goepferich A. 2009. Dimethylether as Novel Solvent for Injectable In Situ Forming Depots. Pharm Res 26:2568–2577.

14. Schoenhammer K, Boisclair J, Schuetz H, Petersen H, Goepferich A. 2010. Biocompatibility of an Injectable In Situ Forming Depot for Peptide Delivery. J Pharm Sci 99:4390–4399.

15. Al-Tahami K, Oak M, Singh J. 2011. Controlled Delivery of Basal Insulin from Phase-Sensitive Polymeric Systems After Subcutaneous Administration: In Vitro Release, Stability, Biocompatibility, In Vivo Absorption, and Bioactivity of Insulin. J Pharm Sci 100: 2161–2171.

16. Liu H, Venkatraman SS. 2012. Cosolvent Effects on the Drug Release and Depot Swelling in Injectable In Situ Depot-Forming Systems. J Pharm Sci 101:1783–1793.
17. Astaneh R, Erfan M, Barzin J, Mobedi H, Moghimi H. 2008. Effects of Ethyl Benzoate on Performance, Morphology, and Erosion of PLGA Implants Formed In Situ. Adv Polym Technol 27:17–26.
18. Kranz H, Bodmeier R. 2007. A novel in situ forming drug delivery system for controlled parenteral drug delivery. Int J Pharm 332:107–114.
19. Lambert WJ, Peck KD. 1995. Development of an in-situ forming biodegradable poly-lactide-*co*-glycolide system for the controlled-release of proteins. J Control Release 33:189–195.
20. Al-Tahami K, Meyer A, Singh, J. 2006. Poly lactic acid based injectable delivery systems for controlled release of a model protein, lysozyme. Pharm Dev Technol 11:79–86.
21. Liu H, Venkatraman SS. 2012. Effect of Polymer Type on the Dynamics of Phase Inversion and Drug Release in Injectable In Situ Gelling Systems. J Biomater Sci-Polym Ed 23:251–266.
22. Kilicarslan M, Koerber M, Bodmeier R. 2014. In situ forming implants for the delivery of metronidazole to periodontal pockets: formulation and drug release studies. Drug Dev Ind Pharm 40: 619–624.
23. Ahmed TA, Ibrahim HM, Ibrahim F, Samy AM, Kaseem A, Nutan MTH, Hussain MD. 2012. Development of biodegradable in situ implant and microparticle injectable formulations for sustained delivery of haloperidol. J Pharm Sci 101:3753–3762.
24. Chhabra S, Sachdeva V, Singh S. 2007. Influence of end groups on in vitro release and biological activity of lysozyme from a phase-sensitive smart polymer-based in situ gel forming controlled release drug delivery system. Int J Pharm 342:72–77.
25. Brodbeck KJ, Pushpala S, McHugh A. 1999. Sustained release of human growth hormone from PLGA solution depots. J. Pharm Res 16:1825–1829.
26. Krasko MY, Kumar N, Domb AJ. 2006. Protein and peptide release from in situ gelling polymer. Biomacromolecules 7:2461–2463.
27. Fiume MZ, Panel CIRRE. 2003. Final report on the safety assessment of triacetin. Int J Toxicol 22:1–10.
28. Cleland JL, Lam X, Kendrick B, Yang J, Yang TH, Overcashier D, Brooks D, Hsu C, Carpenter JF. 2001. A specific molar ratio of stabilizer to protein is required for storage stability of a lyophilized monoclonal antibody. J Pharm Sci 90:310–321.
29. Chang LQ, Pikal MJ. 2009. Mechanisms of protein stabilization in the solid state. J Pharm Sci 98:2886–2908.
30. Shenderova A, Burke TG, Schwendeman SP. 1999. The acidic microclimate in poly(lactide-co-glycolide) microspheres stabilizes camptothecins. Pharm Res 16:241–248.
31. Shenderova A, Ding AG, Schwendeman SP. 2004. Potentiometric method for determination of microclimate pH in poly(lactic-co-glycolic acid) films. Macromolecules 37:10052–10058.
32. Vert M, Li S, Garreau H. 1991. More about the degradation of LA/GA-derived matrices in aqueous-media. J Control Release 16:15–26.
33. Vert M, Li SM, Garreau H. 1994. Attempts to map the structure and degradation characteristics of aliphatic polyesters derived from lactic and glycolic acids. J Biomater Sci-Polym Ed 6:639–649.
34. Fu K, Pack DW, Klibanov AM, Langer R. 2000. Visual evidence of acidic environment within degrading poly(lactic-co-glycolic acid) (PLGA) microspheres. Pharm Res 17:100–106.
35. Raman C, McHugh AJ. 2005. A model for drug release from fast phase inverting injectable solutions. J Control Release 102:145–157.
36. McHugh AJ. 2005. The role of polymer membrane formation in sustained release drug delivery systems. J Control Release 109:211–221.
37. Thakur RRS, McMillan HL, Jones DS. 2014. Solvent induced phase inversion-based in situ forming controlled release drug delivery implants. J Control Release 176:8–23.
38. Parent M, Nouvel C, Koerber M, Sapin A, Maincent P, Boudier A. 2013. PLGA in situ implants formed by phase inversion: Critical physicochemical parameters to modulate drug release. J Control Release 172:292–304.
39. Brodbeck KJ, DesNoyer JR, McHugh AJ. 1999. Phase inversion dynamics of PLGA solutions related to drug delivery - Part II. The role of solution thermodynamics and bath-side mass transfer. J Control Release 62:333–344.